An impact study of dropsonde and QuikSCAT wind data on WRF simulations

Fang-Ching Chien
Department of Earth Sciences, National Taiwan Normal University

1. Introduction

There were several strong southwesterly monsoonal flow and typhoon cases in 2006 that had dropsonde observations taken by Taiwanese meteorological society. The collected sounding data, including pressure, winds, and temperature, were used for data assimilation, using the WRF 3-D Var system. Their impacts on WRF simulations for the heavy rainfall events and typhoon cases were examined in this paper. In addition, QuikSCAT winds were assimilated for the same events to study their impact.

Three cases are presented in this paper. The first two are typhoon events: Typhoons Bilis (2006) and Kaemi (2006). The last case is a heavy rainfall event that occurred during the 2006 Mei-yu season.

2. Model results

The model configuration includes two domains with 45- and 15-km horizontal grid spacing and 31 vertical levels. The global analyses from the NCEP GFS were used for the first guess data. The physics used in the simulation included Kain-Fritsch cumulus parameterization scheme, WSM-5 class microphysics scheme, and the YSU PBL scheme.

Figures 1a, b show the locations of 148 traditional soundings and 15 dropsondes that were assimilated into the WRF Var for the Typhoon Bilis (2006) case. These observations were taken at around 1200 UTC 11 July 2006, which was chosen as model initial time. We carried out two simulations for this event. The control run (CNTL) assimilated all the above observations. The NODROP run was the same as CNTL, except that the dropsondes were not included. The result shows that the typhoon track of the CNTL run was closer to the observed one than that of the NODROP (Fig. 1c). The track errors for the CNTL run were smaller than the NODROP run after 30 h, and the differences between the two track errors increased over time, except at 48 h. This indicates that the WRF simulation of typhoon track improved greatly by assimilating the dropsonde observations. In order to determine the factor that contributes to such improvement after assimilating the dropsonde data, we calculate the difference of v-component winds between the two runs by subtracting the winds of the NODROP run from those of the CNTL run. The difference can clearly indicate the impact of the dropsonde data on the simulation. Figure 1d shows a time-height section by averaging horizontally the difference within the box shown in Fig. 1b. It is evident that at initial time the dropsonde data modified the global analysis by decreasing v-wind below 850 hPa, increasing it between 850 and 500 hPa, decreasing it between 500 and 300 hPa, and increasing it above 300 hPa. The difference changed quickly after the model starts. Between 12 and 36 h, the CNTL run had larger southerly wind component than the NODROP below 500 hPa, while smaller above 500 hPa. At 36-60 h, the difference became mostly positive, which indicates that the CNTL run had larger southerly winds. This explained why the track of the CNTL run moved more to the north and was closer to the observation after 36 h (see Fig. 1c).

Figure 2 shows the similar plots for the Typhoon Kaemi case. The initial time was set at 0000 UTC 23 July 2006, during which there were 147 traditional soundings and 14 dropsondes (Figs. 2a, b). All these observations were assimilated in the CNTL run. In the NODROP run, the dropsondes were removed. Similar to Typhoon Bilis, the CNTL run simulated better track than the NODROP run, although both runs had relatively large track errors

(Fig. 2c). The CNTL run had a track located to the north of the NODROP run at early time (18-48 h), and to the south (or west) at later time (after 48 h). The typhoon center of the CNTL run made landfall across the land of Taiwan, while the NODROP run did not. The time-height section of the averaged v-wind difference between the CNTL and NODROP runs presents a good explanation for the above track difference (Fig. 2d). At the model initial time, the difference shows that the dropsonde data in general made v-component wind stronger below 400 hPa, and smaller above. After the spin-up hours, the difference became positive at all layers. After 42 h or so, the difference turned into negative. This indicates that the CNTL run had stronger southerly steering flow before 42 h and northerly flow after 42 h. This difference caused the CNTL to moved more to the north than the NODROP run before 42 h, and more to the west (or south) across Taiwan after 42 h.

During 8-11 June 2006, there was a Mei-yu front passing over Taiwan. The front brought heavy rainfall to the Taiwan area, resulting in severe flooding and mudslides in many mountainous regions. At around 1200 UTC 9 June 2006, 14 dropsonde observations were taken surrounding the island of Taiwan as shown in Fig. 3b. These observations, along with 133 sounding and 179 QuikSCAT wind observations (Figs. 3a, c), were assimilated using WRF Var for the CNTL run. The NODROP run excluded only the dropsonde data and the NOQSCAT run removed solely the QuikSCAT winds during the data assimilation process.

At 0000 UTC 10 June 2006, a northeast- southwest oriented Mei-yu front was located across southern Taiwan. Radar reflectivity shows that strong convection occurred near the Mei-yu front (Fig. 3d). There were two major bands of convection, one over the southern Taiwan Strait, the other slightly to the north. Over land, the convection was enhanced by the terrain, and it brought heavy rainfall, not only to the mountainous region, but also to the lowlands. The front was nearly stationary early and then slowly moved toward southern Taiwan at about 24 h later.

The simulation result at 12 h shows that, compared with Fig. 3d, the NODROP and CNTL runs (Figs. 3e, f) simulated better radar reflectivity pattern than the NOQSCAT run (Fig. 3g). Although the radar reflectivity of the NODROP run was more intense than the CNTL run, the location of the convection band appeared to be slightly to the north of the CNTL run which agreed better with the observation. On the contrary, the results at 36 h indicate that the CNTL and the NOQSCAT runs produced better convection band near the front than the NODROP run (figures not shown). The above findings suggest that with all data assimilated, the WRF model can reproduce better rainfall pattern associated with the Mei-yu front. The QuikSCAT winds can help the simulation during model early hours (e.g., 12 h). However, since they are 2-D wind data at surface only, the influence reduced as integration time increased. On the other hand, the 3-D dropsonde data of wind, pressure, temperature, and humidity can help simulate better frontal location and convective rainband at early hours. Moreover, the positive impact of the data can last longer at least until 36 h.

3. Summary

The above are just some of the preliminary results of the event. More will be done in the future. From the current analyses, several conclusions can be made. First, the dropsonde data can help to simulate better typhoon track, because the steering flow was better captured. Second, by assimilating all dropsone data and QuikSCAT winds, the Mei-yu front and its associated convection band were better simulated, in terms of frontal location and the strength of the convection. The influence of the near-surface QuikSCAT winds was limited at early stage of the simulation, while the impact of the 3-D dropsonde data can last longer.

Acknowledgment

This work is partly supported by National Science Council of Taiwan. Miss Chang-Mei Hsieh completed most of the WRF simulations.

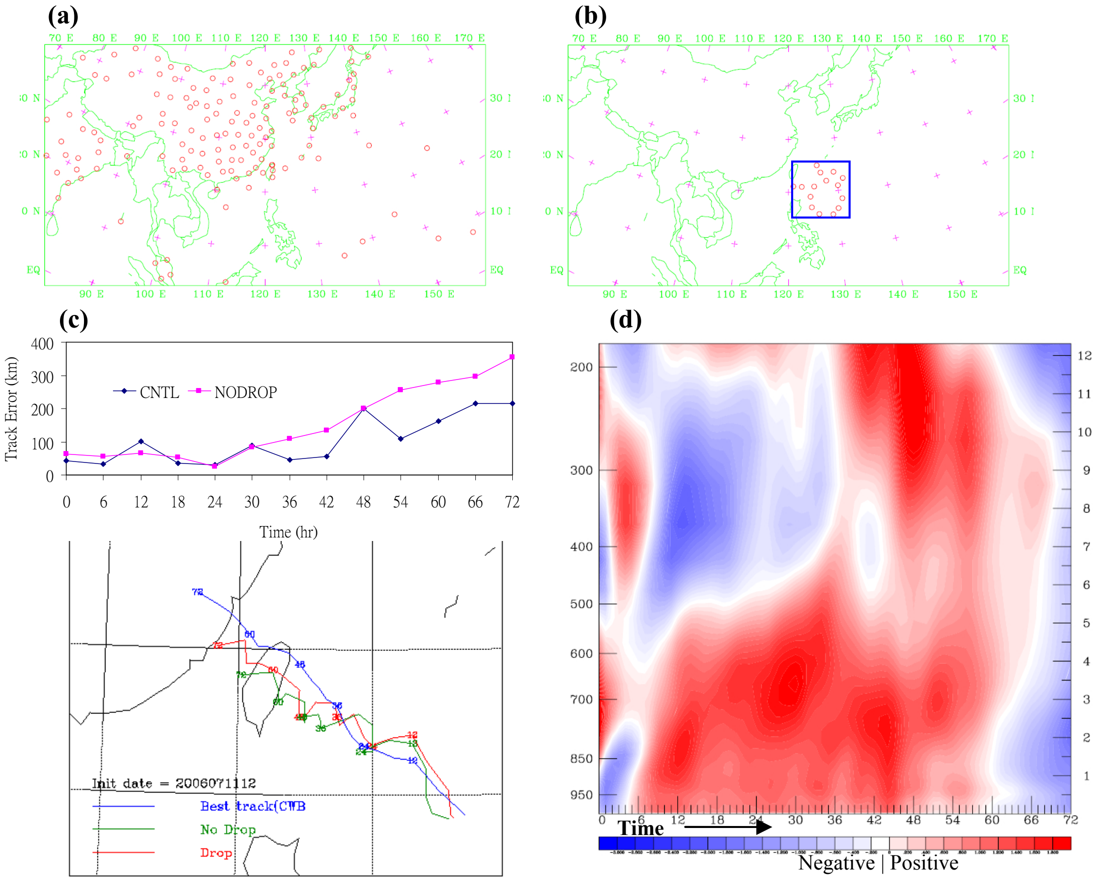

Fig. 1: Typhoon Bilis (2006): (a) Locations of 148 traditional soundings. (b) Locations of 15 dropsondes. (c) Typhoon tracks and track errors for the CNTL and NODROP runs. (d) Time-height section of difference of v-component wind between the CNTL and NODROP runs (CNTL-NODROP) averaged horizontally inside the box shown in b. Red is for positive, and blue is for negative difference.

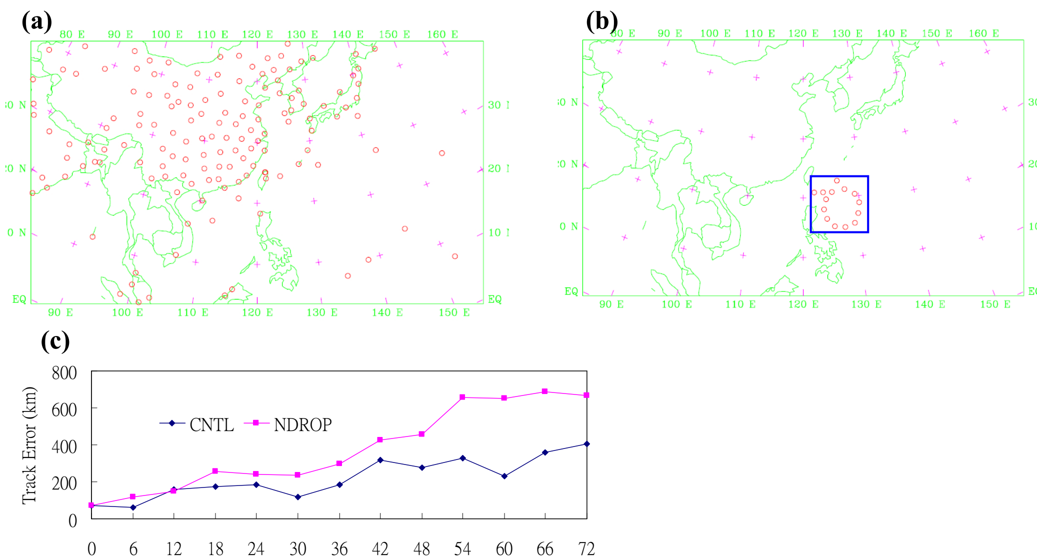

Fig. 2: Same as Fig. 1, except for Typhoon Kaemi.

(c)

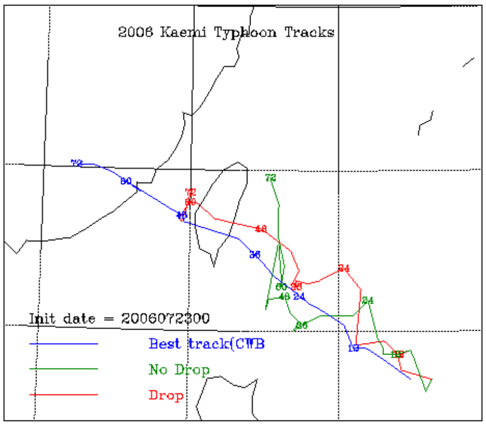

(d)

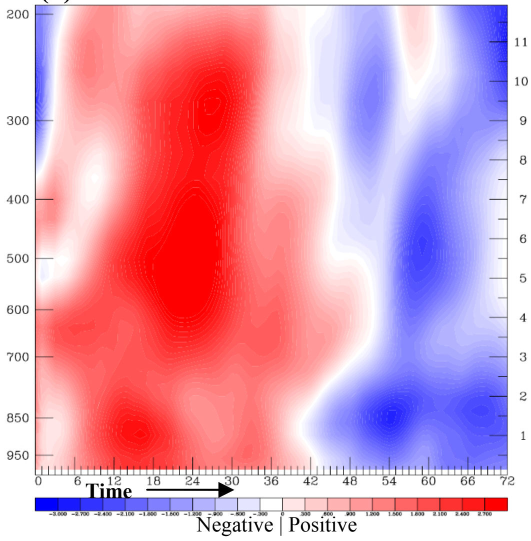

Fig. 2: (Continued)

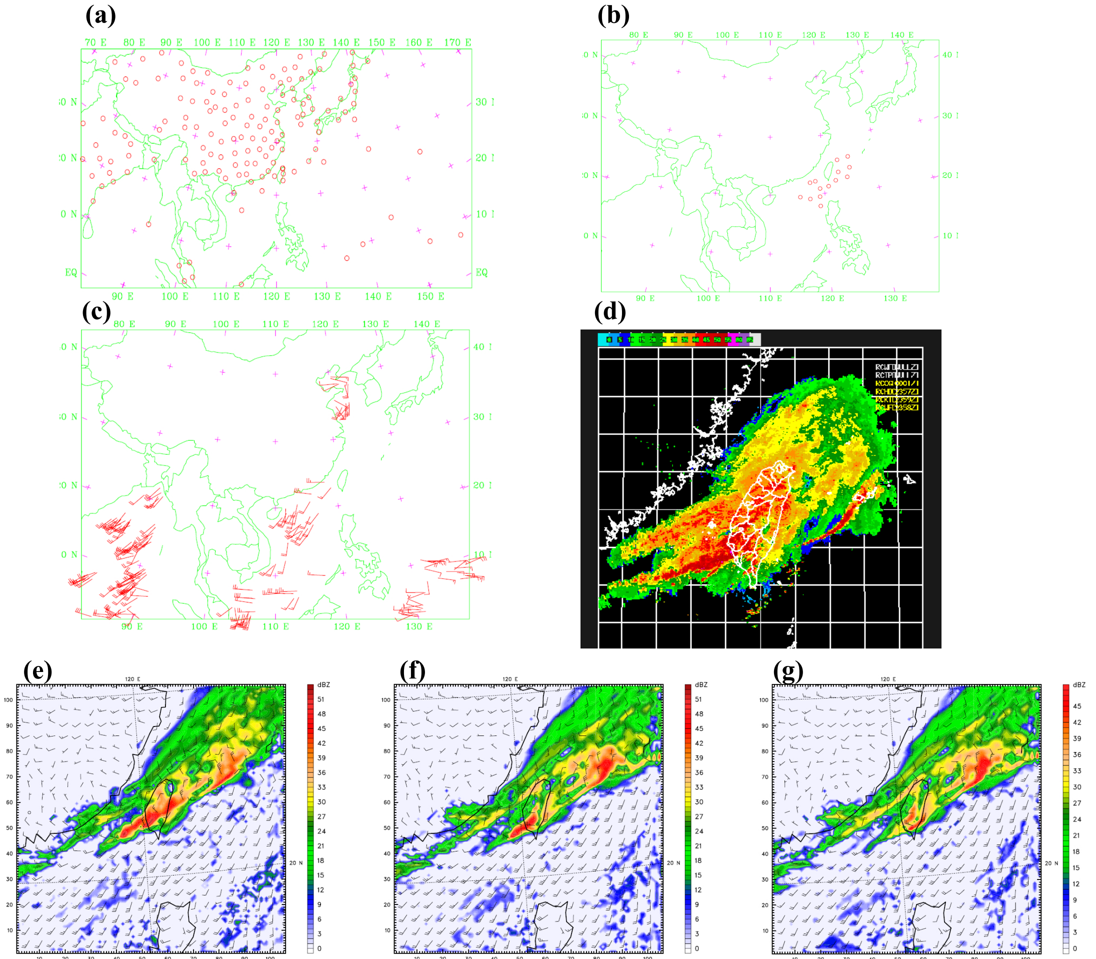

Fig. 3: The Mei-yu front event: (a) Locations of 133 traditional sounding. (b) Location of 14 dropsondes. (c) Locations of 179 QuikSCAT winds. (d) Radar reflectivity at 0000 UTC 10 June 2006. (e) Simulated radar reflectivity at 12 h of the NODROP simulation. (f) Same as e, but for the CNTL run. (g) Same as e, but for the NOQSCAT run.